Surface Structures and Adhesive-Free Adhesion Characteristics of Polyaniline Films after Modification by Graft Copolymerization

Z. F. Li, E. T. Kang,* and K. G. Neoh

Department of Chemical Engineering, National University of Singapore, Kent Ridge, Singapore 119260

K. L. Tan

Department of Physics, National University of Singapore, Kent Ridge, Singapore 119260

C. C. Huang and D. J. Liaw

Department of Chemical Engineering, National Taiwan Institute of Technology, Taipei, Taiwan 106, Republic of China

Received October 28, 1996; Revised Manuscript Received February 4, 1997[⊗]

ABSTRACT: Surface modifications of emeraldine base (EB) films have been carried out via thermally induced graft copolymerization with acrylic acid (AAc), sodium salt of styrenesulfonic acid (NaSS), *N*,*N*′-dimethyl(methacryloylethyl)ammonium propanesulfonate (DMAPS), and acrylamide (AAm). The structure and chemical composition of each graft-copolymerized surface were studied by angle-resolved X-ray photoelectron spectroscopy (XPS). In all cases, the concentration of grafting increases with monomer concentration. Surface grafting with the four functional monomers also leads to a more hydrophilic EB film surface. Two graft-copolymerized EB film surfaces are capable of exhibiting adhesive-free adhesion when brought into direct contact in the presence of water and subsequently dried. This adhesive-free adhesion also exists between a surface-modified EB film and a similarly modified polytetrafluoroethylene (PTFE) film from graft copolymerization. The development of the lap shear adhesion strength depends on the concentration of the surface graft, the adhesion (drying) time, the physical property of the substrate, the microstructure of the grafted surfaces, and the nature of the molecular interaction (dispersive, ionic, etc.) at the junction. Lap shear adhesion strength as high as 340 N/cm^2 was achieved between two EB films graft copolymerized with the amphoteric DMAPS monomer.

Introduction

During the past one-half decades, the synthesis and characterization of electroactive polymers have quickly become one of the most important research areas in polymer science.[1] Among the electroactive polymers, polyaniline (PANI) has been of particular interest because of its ability to exist in a number of intrinsic redox states,[2] of the reversibility of its conductivity,[3] of its environmental stability, and of its high degree of processability.[4,5] The aniline polymers have the general formula $[(-B-NH-B-NH)_y(B-N=Q=N-)_{1-y}]_x$, where B represents a benzenoid ring while Q represents a quinonoid ring. The intrinsic oxidation state of the polymer can be varied from the fully reduced state ($y = 1$) to the fully oxidized state ($y = 0$). The 50% intrinsically oxidized state has been termed emeraldine base (EB).[6] The EB is soluble in *N*-methylpyrrolidinone (NMP) and can be cast into film from its solution. The fact that the electrical properties of the PANI can be varied by controlled "doping" (oxidation/reduction or protonation/deprotonation), as well as by varying the type of anions incorporated, suggests that they can be used as active materials for electrodes and sensors. With respect to these applications, material modification and functionalization, in particular those aiming at the surface, will be necessary. The general methods of chemical modification of polymer surfaces have been reviewed recently.[7] It has also been demonstrated that surface modification can be performed through graft copolymerization under mild conditions for a number conventional polymers, such as polyethylene (PE), poly(ethylene terephthalate) (PET), polycarbonate (PC), and polytetrafluoroethylene (PTFE), etc., when their surfaces are pretreated with high-energy radiation, plasma, corona discharge, ozone exposure, or ultraviolet (UV) irradiation.[8−10] The surface-modified polymer substrates can be further functionlized through protein and enzyme immobilization.[11,12] In addition, their improved hydrophilic and adhesion properties after graft copolymerization have also been of recent interests.[13,14]

Because electroactive polymer substrates may provide an added advantage over conventional polymer substrates, it should be interesting to extend the study to the surface-modified and functionalized electroactive polymers.[15] The present work involves the investigation of surface modifications of PANI film by graft copolymerization with acrylamide (AAm), acrylic acid (AAc), *N*,*N*′-dimethyl(methacryloylethyl)ammonium propanesulfonate (DMAPS), and the sodium salt of 4-styrenesulfonic acid (NaSS). The effect of monomer concentration used during graft copolymerization on the copolymer composition and surface microstructure was studied by angle-resolved X-ray photoelectron spectroscopy (XPS). The adhesive-free adhesions between two surface graft copolymerized PANI films and between a surface graft copolymerized PANI film and a surface graft copolymerized polytetrafluoroethylene (PTFE) film were also studied in some detail. The latter approach parallels that of the surface modification of fluoropolymer by other physicochemical means for improving the adhesion of electroactive polymer coatings.[16] Because of the reactive and somewhat oxidized nature of the

* To whom correspondence should be addressed: Fax (65) 779-1936; E-mail, cheket@leonis.nus.sg.

[⊗] Abstract published in *Advance ACS Abstracts,* May 1, 1997.

S0024-9297(96)01595-1 CCC: $14.00

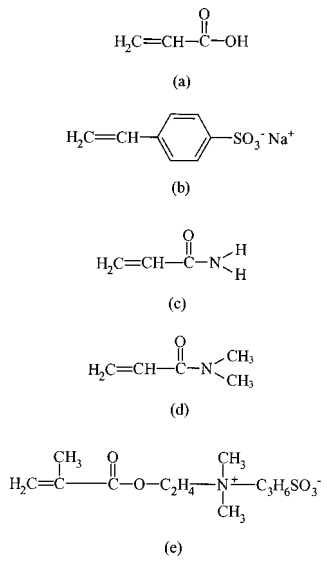

Figure 1. Molecular structures of the five monomers used for graft copolymerization: (a) AAc, (b) NaSS, (c) AAm, (d) DMAA, and (e) DMAPS.

conjugated polymer surfaces, as well as the thermal stability of PANI (stable to 150 °C),[17] the graft copolymerization can be accomplished thermally and in the absence of any surface pretreatment or preactivation of the PANI films. Common pretreatment methods, such as ozone and Ar plasma pretreatment, have been known to result in overoxidation and structural alteration of the PANI chains at the film surface.[18,19]

Experimental Section

Materials. The monomers used for graft copolymerization, such as acrylic acid (AAc), sodium salt of 4-styrenesulfonic acid (NaSS), and acrylamide (AAm), were obtained from Wako Pure Chemical Industries, Ltd. of Tokyo, Japan. The *N*,*N*′-dimethyl(methacryloylethyl)ammonium propanesulfonate (DMAPS) amphoteric monomer was prepared according to the method reported earlier.[20] Cationic monomer, *N*,*N*′-dimethylacrylamide (DMAA) was also used for graft copolymerization on polytetrafluoroethylene (PTFE) film. The molecular structures of the five monomers used for graft copolymerization are shown in Figure 1. PTFE film having a thickness of about 0.01 cm was purchased from Goodfellow, Inc. of Cambridge, U.K. The solvents and other reagents were of reagent grade and were used without further purification.

Polyaniline Film. Emeraldine salt was prepared by the oxidative polymerization of aniline by ammonium persulfate in 1 M HCl according to the method reported in the literature.[3] It was converted to neutral emeraldine base (EB) by treatment with excess 0.5 M NaOH and dried by pumping under reduced pressure. Free standing and lightly cross-linked EB film was prepared by heating the concentrated *N*-methylpyrrolidinone (NMP) gel solution (containing 8% EB by weight) at 150 °C for 6 h, followed by exhaustive pumping under reduced pressure. The EB film so prepared has a tensile yield strength of about 120 N/cm^2.

Graft Copolymerization. EB film strips of about 2.0 cm × 4.0 cm were used in all grafting experiments. In the case of graft copolymerization with AAc, each EB film was immersed in an aqueous AAc solution of a predetermined concentration in a Pyrex glass ampule. The reaction mixture was thoroughly degassed with N_2 and subsequently sealed with a silicon rubber stopper. The reaction mixture was then kept in an 80 °C water bath for about 1 h. After each grafting experiment, the EB film was removed from the viscous homopolymer solution and washed with a jet of double-distilled water. It was then immersed in a room-temperature water bath with continuous stirring for at least 48 h to remove the residual homopolymer. Similar procedures were also used for the graft copolymerization with NaSS, AAm, and DMAPS monomers. In the case of surface modification of PTFE films, the inert fluoropolymer substrate was first pretreated with Ar plasma, followed by near-UV-light-induced graft copolymerization with AAc or DMAA, according to the method reported earlier.[10,21]

Surface Characterization after Graft Copolymerization. The polymer films after graft copolymerization were characterized by contact angle measurements and XPS. Advancing and receding contact angles were measured by the angle-of-tilt method at 25 °C and 70% relative humidity, using a telescopic goniometer (Ramehart, Model 100-00-(230)). The telescope with a magnification power of 23× was equipped with a protractor of 1° graduation. The angles reported were accurate to within ±3°. For each film, at least three measurements on different surface locations were averaged.

XPS measurements were made on a VG ESCALAB MkII spectrometer with a Mg Kα X-ray source (1253.6 eV photons). The X-ray source was run at a reduced power of 120 W (12 kV and 10 mA). The polymer films were mounted on the standard VG sample studs by means of double-sided adhesive tape. The core-level spectra were obtained at different photoelectron takeoff angles (α, with respect to the film surface), ranging from 20° to 75°. The pressure in the analysis chamber was maintained at 10^{-8} mbar or lower during the measurements. To compensate for surface charging effects, all binding energies were referenced to the C1S neutral carbon peak at 284.6 eV. In peak synthesis, the line width (full width at half maximum or fwhm) of Gaussian peaks was maintained constant for all components in a particular spectrum. Surface elemental stoichiometries were determined from peak area ratios, corrected with the experimentally determined sensitivity factors, and is liable to ±5% error. The sensitivity factors were determined using binary compounds of well-defined stoichiometries. The concentrations of surface-grafted AAc, AAm, and NaSS polymers are expressed as the [*C*OOH]/[N], [H_2N*C*=O]/[N], and [S]/[N] ratios, as reported previously for the near-UV-light-induced graft copolymerization.[15] The surface concentration of the grafted DMAPS polymer, on the other hand, is expressed as the ratio of [N^+]/([=N−]+[−NH−]) derived from the curve-fitted N1S core-level spectrum.

Adhesion Strength Measurements. Adhesive-free adhesion was achieved by lapping two graft copolymerized strips together in the presence of 5 μL of deionized water and under a constant load of 21 N at room temperature and 70% relative humidity. The lapping area of the two graft copolymerized films was kept at 5 mm × 5 mm, unless otherwise stated. After a fixed adhesion (drying) time, the adhesion strength was determined by measuring the lap shear adhesion force using a microprocessor controlled Rheometrics Miniature Materials Tester (UK). All measurements were carried out at a crosshead speed of 10 mm/min. For each lap shear strength reported, at least three sample measurements were averaged.

Result and Discussion

Surface Graft Copolymerization. Previous XPS studies[22,23] have shown that the quinonoid imine (=N− structure), benzenoid amine (−NH− structure), and positively charged nitrogen in a polyaniline (PANI) complex correspond respectively to N1S peak components with binding energies (BEs) at about 398.2, 399.4, and >400 eV in the properly curve-fitted N1S core-level spectrum. Figures 2a,b show, respectively, the C1S and N1S core-level spectra of the lightly cross-linked EB film used in the present study. The film consists of about equal amounts of imine and amine nitrogens, consistent with the intrinsic redox state of EB. The residual high-BE components above 400 eV in the N1S core-level spectrum may have resulted at least in part from surface oxidation products or weakly charge-transfer-complexed oxygen,[22] as well as interchain hydrogen bonding in thermally induced PANI aggregates.[24]

Figures 3a−d show, respectively, the C1S and N1S core-level spectra, obtained at two takeoff angles of 75°

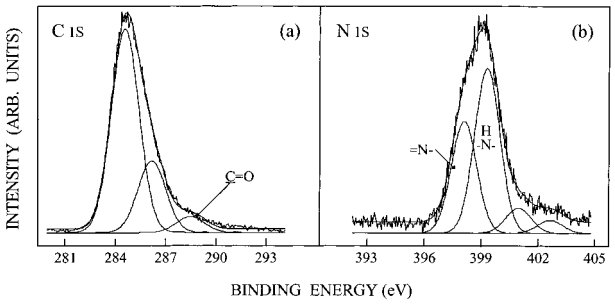

Figure 2. C1S and N1S core-level spectra for a pristine (untreated) EB film.

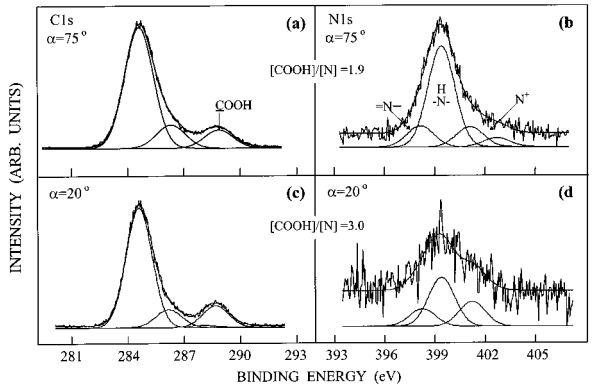

Figure 3. C1S and N1S core-level spectra acquired at takeoff angles of (a and b) 75° and (c and d) 20° for an EB film after thermally induced graft copolymerization in 10 wt % AAc solution.

and 20° for an EB film after thermal graft copolymerization in 10 wt % AAc monomer solution. The small but distinct high-BE C1S component at about 288.7 eV is characteristic of the carboxylic acid group of a grafted AAc polymer.[25] The appearance of this component confirms the presence of a surface-grafted AAc polymer. The amount of the grafted AAc polymer at the surface can be readily determined from the corrected area ratio of the C1S peak component at 288.7 eV and the total N1S core-level spectral area and can be expressed as the [COOH]/[N] ratio. The enhanced N1S high-BE tail above 400 eV and the reduction in the proportion of the imine component at 398.2 eV suggest that graft copolymerization with AAc readily results in a self-doped or self-protonated EB surface. A significant proportion of the imine nitrogen in this sample, however, remains unprotonated, even at a [COOH]/[N] ratio as high as 3.0. Thus, steric hindrance and the chain conformation of the grafted AAc polymer must have played an important role in the protonation of the EB surfaces. The fact that the grafted AAc polymer exists predominantly at the surface region of the EB film is readily revealed by core-level signals acquired at different takeoff angles (takeoff angles of 20° and 75°). For core-level signals obtained at the more surface-glancing angle of 20°, a significantly higher [COOH]/[N] ratio is observed. The fact that grafting occurs predominantly at the top surface of the EB film is consistent with the lack of chain mobility arising from the lightly cross-linked nature of the EB film. Graft copolymerization with the hydrophilic monomer has also given rise to a very hydrophilic EB film surface.

Similarly, the respective C1S and N1S core-level spectra, obtained at takeoff angles of 75° and 20°, for the 10 wt % AAm graft copolymerized EB film are shown in Figures 4a−d. The presence of a surface-

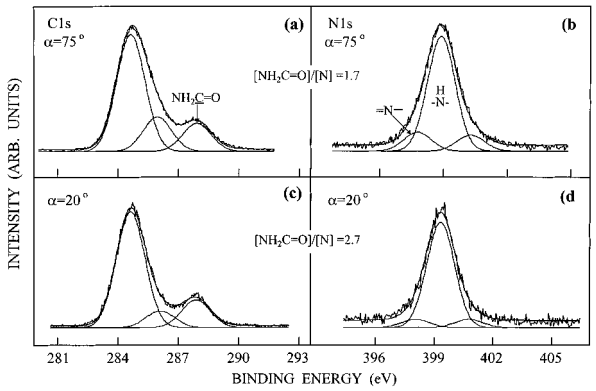

Figure 4. C1S and N1S core-level spectra acquired at takeoff angles of (a and b) 75° and (c and d) 20° for an EB film after thermally induced graft copolymerization in 10 wt % AAm solution.

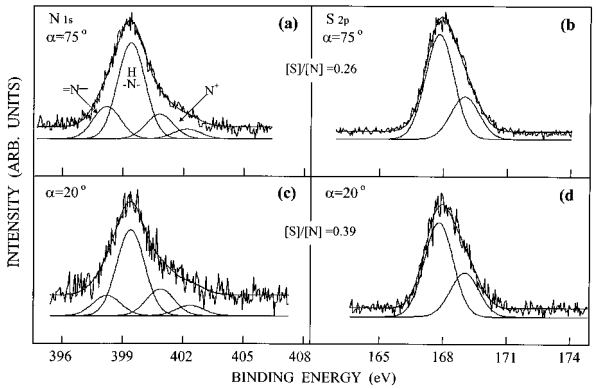

Figure 5. N1S and S2P core-level spectra acquired at takeoff angles of (a and b) 75° and (c and d) 20° for an EB film after thermally induced graft copolymerization in 10 wt % NaSS solution.

grafted AAm polymer is readily suggested by the substantially enhanced C1S high-BE component at about 287.8 eV, attributable to the carbonyl group of the AAm polymer.[25] It is also indicated by a substantial increase in the intensity of the N1s core-level component at 399.4 eV, owing to the contribution from the $-NH_2$ structures of the grafted AAm polymer. This N1S component of the AAm polymer coincides with that of the amine nitrogen of the EB. Figures 4a−d readily suggest that a significant extent of AAm polymer grafting has been achieved. The amount of surface-grafted AAm polymer can be estimated by comparing the $H_2NC{=}O$ component area at 287.8 eV in the C1S core-level spectrum and the area of the main neutral C1S peak at 284.6 eV, taking into account of the fact that each AAm unit has three carbon atoms while each aniline unit has six carbon atoms. Again, a comparison of the core-level signal intensities acquired at different takeoff angles of 75° and 20° suggests that graft copolymerization occurs mainly at the EB surface, as revealed by a higher $[H_2NC{=}O]/[N]$ ratio and the considerable decrease in the proportion of the imine nitrogen component in the N1S spectrum of the EB film at the more surface glancing angle of 20°.

Figures 5a−d show, respectively, the N1S and S2P core-level spectra for an EB film after surface graft copolymerization with NaSS. The presence of the surface-grafted styrenesulfonic acid polymer (as no Na1S core-level signal was detected) is clearly suggested by the appearance of the S2p core-level signal at about 168.0 eV, characteristic of the covalently bonded sulfonic acid group ($-SO_3^-$) of the styrenesulfonic acid poly-

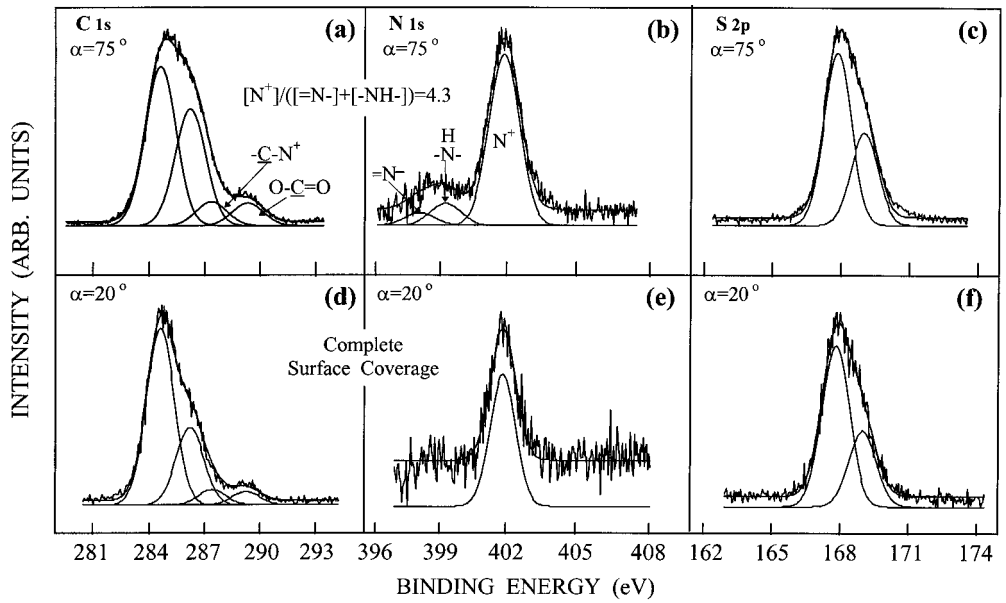

Figure 6. C1S, N1S, and S2P core-level spectra acquired at takeoff angles of (a to c) 75° and (d to f) 20° for an EB film after thermally induced graft copolymerization in 1 wt % DMAPS solution.

mer.[25] In this case, the surface composition or the concentration of surface grafting can be conveniently determined from the sensitivity factor corrected [S]/[N] spectral area ratios. In comparison with the graft copolymerization of AAc and AAm, the low [S]/[N] ratio suggests the presence of a substantially lower graft copolymerization efficiency for NaSS under the same experimental conditions. However, similar to the case of the AAc graft copolymerized surface, the N1S spectra of the styrenesulfonic acid polymer grafted samples all show the presence of a high BE tail above 400 eV and a lower N1S component intensity at 398.2 eV compared to that of the pristine EB film. These results readily suggest that the sulfonic acid groups of the grafted polymer must have also participated in the protonation of the imine nitrogens of the EB to give rise to a self-protonated or self-doped EB surface.

Figures 6a−f show the respective C1S, N1S, and S2P core-level spectra of an EB film, obtained at takeoff angles of 75° and 20°, after thermal graft copolymerization in 1 wt % aqueous DMAPS monomer solution. The DMAPS polymer has a C1S component at a BE of about 287.0 eV, which is attributed to the $-C-N^+$ functional group.[25] Also, the appearance of the S2P core-level signal at about 168.0 eV, characteristic of the covalently bonded sulfonic acid group ($-SO_3^-$) of the DMAPS polymer, is consistent with the presence of surface-grafted DMAPS polymer. In the case of the N1S spectrum, the $-C-N^+$ groups of the grafted DMAPS polymers give rise to a distinct N^+ nitrogen component at a BE of about 401.7 eV. The amount of the grafted DMAPS polymer on the EB substrate can be determined from the N1S core-level spectral component areas and expressed as the $[N^+]/([=N-]+[-NH-])$ ratio. From Figure 6e, it can be seen that the concentration of the grafted DMAPS polymer is so high that the N1S spectrum is dominated by the N^+ component of the DMAPS polymer. This result suggests the presence of total surface coverage of the EB film by the grafted DMAPS chains. Nevertheless, from the comparison of the N1S line shapes in Figures 6b,e, it can also be conclude that the grafted DMAPS polymer exists mainly at the outer surface of the EB film. For DMAPS concentration above 1 wt %, the N1S spectra of the graft-copolymerized surfaces show only the N^+ component at both photoelectron takeoff angles. These results imply that the surface of the EB film has been completely covered by a layer of the DMAPS polymer with thickness exceeding the probing depth (in the order of about 50 Å at $\alpha = 75°$) of the XPS technique.[26,27] Table 1summarized the results of graft copolymerization with DMAPS at different monomer concentrations. Thus, graft copolymerization with DMAPS proceeds with much higher efficiency than the graft copolymerizations with AAc, AAm, or NaSS under similar experimental conditions.

Table 1. Extent of Surface grafting, Derived from Two α's of 75° and 20°, for the DMAPS-Graft-Copolymerized PANI Films at Different Monomer Concentrations

	surface graft concentration of DMAPS	
concn	α = 75°	α = 20°
1% DMAPS	4.3	cc
2.5% DMAPS	cc[a]	cc
5% DMAPS	cc	cc
10% DMAPS	cc	cc

[a] cc = Complete coverage; no PANI chain was detected.

The concentrations of surface-grafted AAc, AAm, and styrenesulfonic acid polymers as a function of the respective monomer concentrations used during graft copolymerization at 80 °C for 1 h are shown in Figures 7a−c respectively. The grafting concentrations expressed as the corresponding [*C*OOH]/[N], [H_2N*C*=O]/[N], and [S]/[N] ratios at the two takeoff angles are also compared. In general, the concentrations of the grafted AAc AAm and styrenesulfonic acid polymer increase with increasing monomer concentration in the reaction media. In all cases, the concentrations of the surface-grafted polymers become saturated at monomer concentrations above 10 wt %. The microstructure of the surface after graft copolymerization is clearly revealed by the angle-dependence XPS surface compositions in Figure 7. In all the cases, graft copolymerization occurs mainly at the EB surface and there is only limited penetration of the graft chains into the subsurface layer, unlike those observed during the surface graft copolymerization of polytetrafluoroethylene (PTFE) films (see below) and other thermoplastic films.[21,28] The grafted

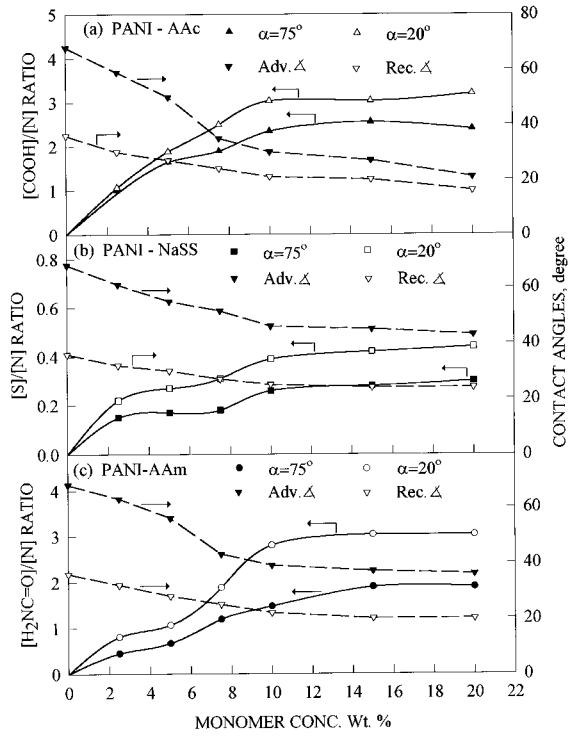

Figure 7. Effect of monomer concentration on the amount of surface-grafted (a) AAc, (b) NaSS, and (c) AAm polymer on EB films. The contact angles of the corresponding graft-copolymerized surface are also shown.

chains also gives rise to a more hydrophilic EB surface. The acquired hydrophilic property of the modified surfaces is indicated by the significant decreases in both the advancing and receding water contact angles (Figure 7). Also, with the increasing amounts of grafted Aac, styrenesulfonic acid, or AAm polymer, the advancing and receding contact angle hysteresis of the EB film also becomes less pronounced.

The fact that graft copolymerization has actually occurred on the EB film surface is further confirmed by the presence of a strong adhesive-free adhesion strength at the lapped junction between two surface modified EB films (see next section). As the adhesive-free adhesion strength arises to a large extent from the time-dependent chain diffusion and entanglement at the lapped junction, the phenomenon cannot be accounted for by the simple surface derivatization of the EB films. The fact that graft copolymerization is limited mainly to the film surface is readily suggested by the complete lack of bulk conductivity for EB films with a substantial amount surface grafted polymeric acid chains. The latter films only exhibit a semiconductive surface as a result of protonation of PANI chains at the surface by the grafted polymeric acid (see Figures 3 and 5). Furthermore, the cross-linked nature of the EB film will prevent any significant diffusion of the surface grafted chains into the bulk phase.

Our earlier studies[10,21] have shown that the Ar plasma pretreated PTFE films are susceptible to further surface modification by near-UV-light-induced graft copolymerization with AAc and DMAA. Figures 8a,b show the C1S core-level spectra, obtained at takeoff angles of 20° and 75°, respectively, for a 5-s Ar plasma pretreated PTFE film after graft copolymerization in 10% AAc solution. In all cases, the graft yield increases with plasma pretreatment time, as shown in Figures 9a,b, respectively, for the AAc- and DMAA-graft-copolymerized PTFE surfaces. The surface concentra-

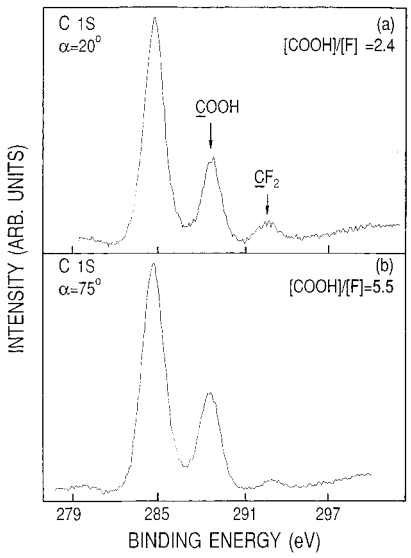

Figure 8. Angular-dependent C1S core-level spectra for a 5-s Ar plasma pretreated PTFE film after near-UV-light-induced graft copolymerization in 10 wt % AAc solution (near-UV illumination time = 0.5 h).

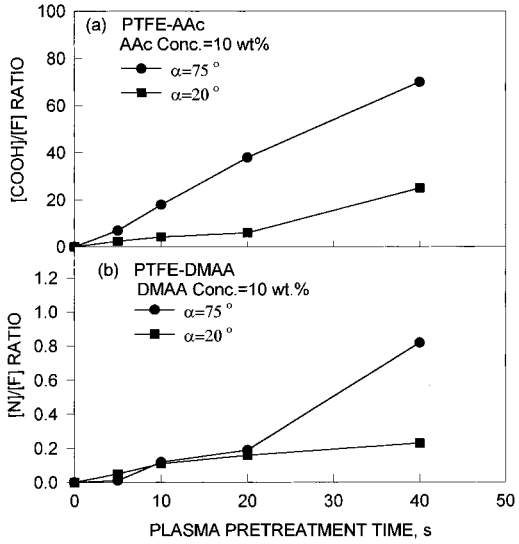

Figure 9. Effect of Ar plasma pretreatment time on the amount of surface-grafted (a) AAc and (b) DMAA polymer on PTFE films.

tions of the grafted AAc and DMAA polymers were expressed simply as the [COOH]/[F] and [N]/[F] ratios, respectively, and were determined from the XPS-derived surface stoichiometries. This ratios can be readily converted to the number of repeating units of the PTFE chain by taking into account of the fact that there are four fluorine atoms per repeating unit of the PTFE chain. The angular-dependent XPS results of Figures 8 and 9 readily suggest that a stratified surface microstructure with a significant higher substrate to graft chain ratio in the top surface layer than in the subsurface layer is always obtained for the PTFE surface with a substantial amount of grafted hydrophilic chains. This microstructure is a result of "surface restructuring" to minimize the surface free energy after graft copolymerization. The hydrophilic graft chains in the subsurface region, however, readily revert to the top surface upon rehydration of the film, as evidenced by the contact angle data.[21]

Adhesive-free Adhesion Between PANI Films. The lap shear adhesion strength between two identically

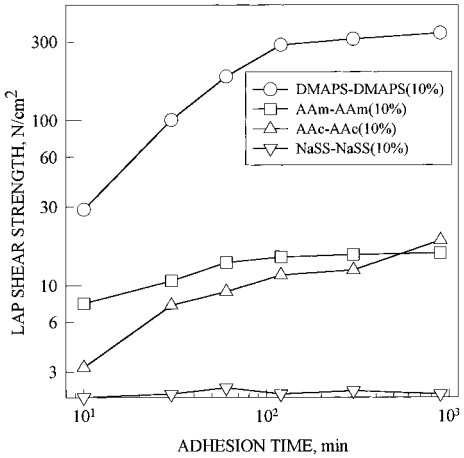

Figure 10. Comparison of lap shear adhesion strength at break between two identical AAc-, AAm-, NaSS-, and DMAPS-graft-copolymerized PANI films as a function of adhesion (drying) time.

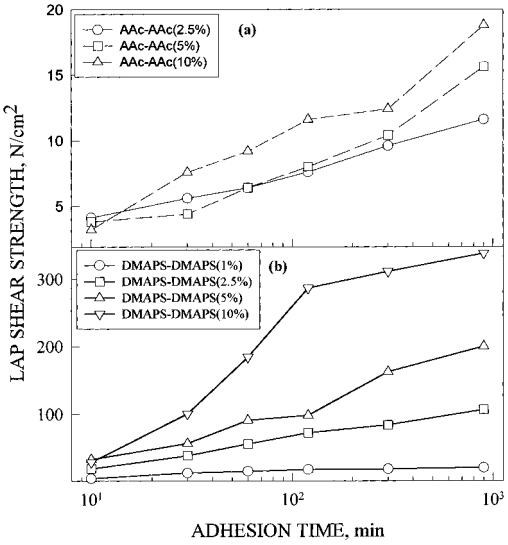

Figure 11. Lap shear adhesion strength at break between two identical (a) AAc-, and (b) DMAPS-graft-copolymerized PANI films as a function of adhesion (drying) time and graft concentration.

modified EB films from graft copolymerization with AAc, NaSS, AAm, and DMAPS were measured after a fixed period of drying (adhesion). The lap shear adhesion strengths are plotted against adhesion time in Figure 10 for the four types of surface-modified EB films from graft copolymerization in 10 wt % of the respective monomer solution. The respective graft concentrations correspond to those reported in Figure 7 and Table 1. With the exception of the NaSS-graft-copolymerized films, the adhesion strengths increase monotonically with adhesion time in the other three cases. In the case of the DMAPS-graft copolymerized EB films with 300 min of adhesion time, the adhesion strength reaches to about 340 N/cm^2. The AAc- and AAm graft-copolymerized EB films of lap shear adhesion strengths are far below that observed between two DMAPS-graft-copolymerized films. The relatively low lap shear adhesion strengths between two NaSS-graft-copolymerized films can be attributed to the relatively low extent of surface graft copolymerization, as the adhesion process depends on the extent of chain entanglement, the graft concentration, and the microstructure of the grafted layer.[21,29]

The adhesion process can be defined in terms of microscopic interactions at an interface[30] and is related to the sum of all the intermolecular interactions at the interface. Voyutskii[31] proposed a diffusion theory that provides a good explanation of the adhesion phenomenon. According to this theory, after the intimate contact is established between two nonporous polymer surfaces, the segments of the polymer chains diffuse across the interface and the adhesion is related to the extent of interdiffusion and chain interpenetration across the polymer−polymer interface. From this theory, it may be possible to characterize the adhesion-free adhesion between two graft-copolymerized polymer films as a multistage process. First, the grafted hydrophilic polymer on the surface of the EB film swells or dissolves in the presence of water to form an interface substrate between the two contacting films. Then the grafted molecular segments migrate or diffuse in the aqueous environment from one surface domain into another and in the process entangle with one another due to micro-Brownian motion. Finally, the water evaporates and the diffused chains contract and strongly entangled with each other. Thus, the adhesion strength intensified. It is expected that the surface microstructure, the surface morphology, the interfacial charge-transfer interaction, and the property of the substrate may play an important role in the observed interfacial adhesion strength.

The observed lap shear adhesion between two similar EB films graft copolymerized with AAc, AAm, NaSS, and DMAPS can be explained by the above theory. Among the four types of the modified substrates, the DMAPS-polymer-grafted films show the highest adhesion strength. One reason is that the DMAPS-graft-copolymerized substrate has a high grafted concentration, as revealed by the XPS results in Table 1. Furthermore, the lap shear adhesion strength in the case of DMAPS graft-copolymerized films is further enhanced by the strong interchain electrostatic interaction arising from the amphoteric nature (i.e., containing both the CN^+- and the $-SO_3^-$ species)[20] of the grafted DMAPS polymer. Because the electrostatic interaction is less dependent on chain diffusion and entanglement, as well as on the presence of water at the interface, respectable lap shear adhesion strength developed immediately after the two DMAPS-graft-copolymerized films are brought into contact. A lap shear adhesion strength of about 30 N/cm^2 was achieved after 10 min of interfacial contact. The lower adhesion strength between two identical AAc- or AAm-graft-copolymerized films is due to the lack of electrostatic interaction. Because of the rigidity of the present cross-linked EB film, the efficiency of intimate interfacial contact between the two EB films is substantially reduced. The reduction in intimate contact will have an effect on the interdiffusion and entanglement of the grafted chains between the two substrates. The effect becomes prominent especially when the concentration of the grafted polymer chains is low, as in the case of NaSS-graft-copolymerized surfaces.

The effect of the grafted AAc and DMAPS polymer concentrations on the adhesion-free adhesion strength of the EB films is shown in Figure 11. In each case, the adhesion strength increases with increasing graft concentration as a result of the increase in graft chain interaction and entanglement. With a lower concentration of grafted polymer on the EB film, the lap shear adhesion strengths level off at shorter adhesion time. In the case of AAc-graft-copolymerized films, the adhe-

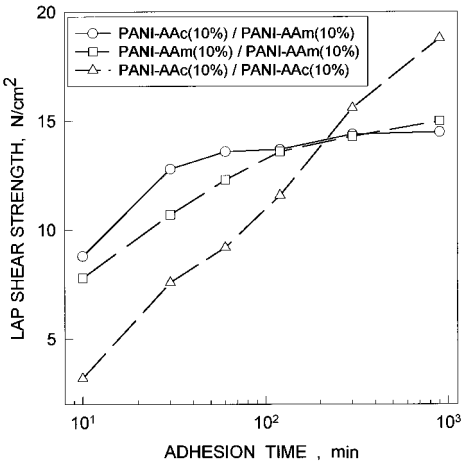

Figure 12. Lap shear adhesion strength at break for interfaces formed between AAc and AAm-, between AAc and AAc-, and between AAm and AAm-graft-copolymerized-PANI films.

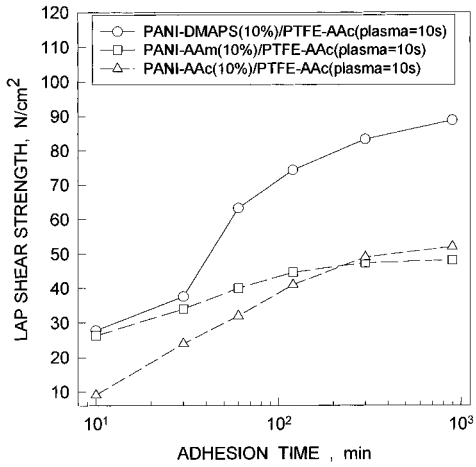

Figure 13. Lap shear adhesion strength at break for interfaces formed between AAc (PANI) and AAc (PTFE)-, between AAm (PANI) and AAc (PTFE)-, and between DMAPS (PANI) and AAc (PTFE)-graft-copolymerized films.

sion strength of films with lower graft concentration is higher at shorter adhesion time. As the adhesion time increases, the adhesion strengths of the films with higher graft concentrations increase more rapidly than the adhesion strength of the film with a lower graft concentration. This phenomenon may be attributed to the effect of surface microstructure and the strong water retention ability of the AAc polymer, especially at the high graft concentration.[21] In the case of DMAPS-graft-copolymerized films, the adhesion strength is further enhanced by the amphoteric ionic interactions. The adhesion strength between the two DMAPS-graft-copolymerized films is so high that the 1 wt % monomer-graft-copolymerized films already exhibit a comparable adhesion strength to that between two 10 wt % AAc-graft-copolymerized EB films.

When an AAc-graft-copolymerized EB film was brought into contact with an AAm-graft-copolymerized EB film under load, the films adhered to each other almost instantaneously. The time dependence of the lap shear adhesion strength for the 10 wt % AAc−10 wt % AAm-, 10 wt % AAm−10 wt % AAm-, and 10 wt % AAc−10 wt % AAc-graft-copolymerized film pairs are compared in Figure 12. It can been seen that, at the initial stage, the AAc−AAm pair has the highest adhesion strength, in comparison with the adhesion strengths of the AAc−AAc pair and AAm−AAm pair. However, its strength increases at a slower rate than the adhesion strengths of other two. These observations are attributable to the fact that the interaction between the amine function group of AAm and the carboxyl group of the AAc leads to an electrostatic interaction,[14] in addition to chain diffusion and entanglement. The electrostatic interaction is prominently especially in the initial stage of adhesion. After a long enough contact time, chain entanglement is another important factor contributing to the observed adhesion strength. Thermodynamically, the diffusion of graft molecules or segments from one substrate into another is due to nothing else than their miscibilities in solution. The solution of the two materials is most likely to occur when they are miscible or have similar solubility parameters. Therefore, the electrostatic interaction may contribute to the development of adhesion strength especially in the initial stage before chain diffusion and entanglement become fully established. With the increase in adhesion time, the lower miscibility between the AAc−AAm pair than the miscibilities between the AAc−AAc and AAm−AAm pairs becomes predominant and may actually weaken the graft chain migration and entanglement. As a result, the overall final adhesion strength is not enhanced by electrostatic interaction.

Adhesive-free Adhesion Between PANI and PTFE Films. It is also important to study the adhesion of an electroactive polymer film to other conventional polymer films. The AAc-graft-copolymerized polytetrafluoroethylene (PTFE) film was first selected because of its importance as a dielectric polymer and because of its physical and chemical inertness. Figure 13 gives the adhesive-free adhesion results of the AAc, AAm, and DMAPS graft copolymerized EB films with the AAc-graft-copolymerized PTFE films. The adhesion strength of AAc- or AAm-graft-copolymerized EB film with the AAc graft copolymerized PTFE is higher than that of the corresponding EB film pair. When the stiff EB film is in contact with the soft thermoplastic PTFE film under load, a more intimate contact than that between two stiff PANI films is achieved, thus allowing the grafted chains to diffuse across the interface and entangle with one another more effectively. As the adhesion strength between an EB−PTFE film pair is so high, the lapped adhesion area is reduced to only 5 mm × 1 mm so that the lap shear adhesion strength remains below that of the yield strength of the PTFE film (~20 N/cm^2) used. The phenomena that electrostatic interaction between the grafted AAc and AAm chains dominates the observed adhesion strength in the initial stage and that the miscibility of the grafted chains between two AAc-graft-copolymerized surfaces becomes predominant after a long period of time are also discernible. The adhesion strength between the DMAPS-graft-copolymerized EB film and the AAc-graft-copolymerized PTFE film, or the DMAPS(PANI)−AAc(PTFE) pair, is always higher than the adhesion strengths of the AAc(PANI)−AAc(PTFE) or the AAm(PANI)−AAc-(PTFE) pairs. The phenomenon is again attributable to the high concentrations of grafted DMAPS and AAc chains on the PANI and PTFE surfaces, respectively, as well as the amphoteric nature of the DMAPS chains.

When a DMAPS-graft-copolymerized PANI film was brought into direct contact with a DMAA-graft-copolymerized PTFE film, respectable adhesion strength is again observed. However, unlike the DMAPS(PANI)−AAc(PTFE) pair, the corresponding DMAPS(PANI)−DMAA(PTFE) pair shows a lower adhesion strength,

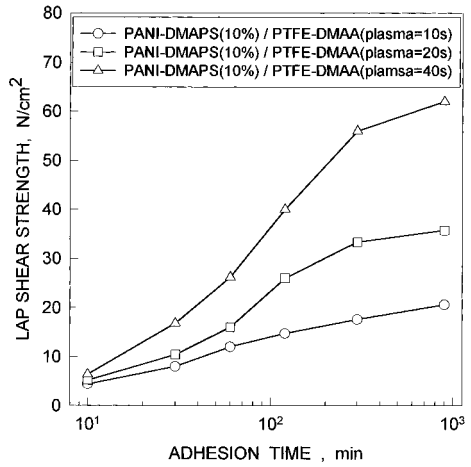

Figure 14. Lap shear adhesion strength at break for interfaces formed between DMAPS (PANI) and of DMAA (PTFE) at various graft concentrations of the DMAA polymer.

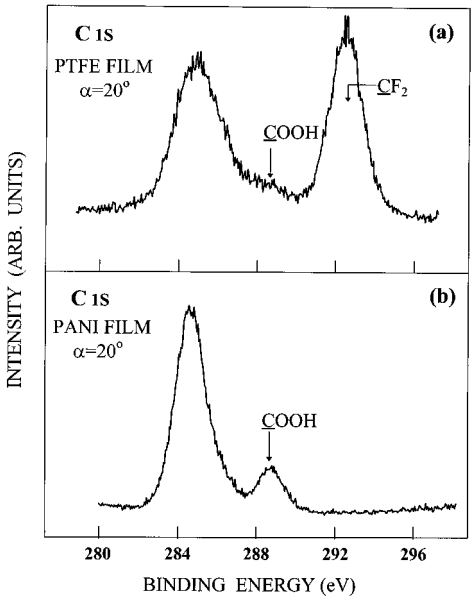

Figure 15. C1S core-level spectra obtained at $\alpha = 20°$ for the delaminated surfaces of (a) the AAc-graft-copolymerized PTFE film and (b)the DMAPS-graft-copolymerized PANI film from the adhesive-free adhesion between the two films (adhesion time = 900 min).

consistent with a lower graft concentration of DMAA chains on the PTFE substrate (see Figure 9). This conclusion is also consistent with the fact that a uniform increase in the lap shear adhesion strength is observed upon increasing the concentration of the grafted DMAA polymer on the PTFE side, as shown in Figure 14. The increase in DMAA polymer concentration in this case is expressed as the increase in plasma pretreatment time, and the graft concentrations correspond to those shown in Figure 9b. At high DMAA polymer concentration, strong adhesion between the two substrates is again observed.

The failure mode of the adhesive-free adhesion between the DMAPS graft copolymerized PANI film and the AAc-graft-copolymerized PTFE film was also inspected, as this heterojunction exhibits a high adhesion strength. Two equal size strips were cut and were lapped together under load for 900 min before been subjected to shear force until the lapped junction delaminated. Figure 15shows the C1S core-level spectra obtained at takeoff angle of 20° for the delaminated PANI and PTFE surfaces. XPS results indicate that for the AAc-graft-copolymerized PTFE film after delamination; there is a sharp decrease in the *C*OOH component intensity at the BEs of 288.7 eV, in comparison with that of the film before the adhesion test (compared with Figure 8). On the other hand, the intensity of the O−*C*═O component in the C1S core-level spectrum of the DMAPS-graft-copolymerized PANI film is significantly enhanced after delamination (compare Figures 15b and 6d). These results readily suggest that the adhesion failure occurs predominantly at the graft−substrate interface of the PTFE film, as a result of extensive chain entanglement and strong charge-transfer interaction among the grafted chains at the lapped junction.

Conclusion

Due to the reactive nature of the conjugated polymer surfaces, EB film without any surface pretreatment is susceptible to surface modification via thermal graft copolymerization with hydrophilic and functional monomers, such as Aac, NaSS, Aam, and DMAPS. Angler-resolved XPS was used to elucidate the surface microstructure and chemical composition of the EB film after graft copolymerization. In all cases, most of the grafted chains are retained at the film surface and the amounts of graft increase with the monomer concentration. It was found that graft copolymerization with AAc and NaSS also gives rise to a self-protonated EB surface structure. Taking into account of the surface microstructure after graft copolymerization, a mechanism involving a multistage process in series has been used to explain the adhesive-free adhesion phenomenon between two graft copolymerized EB films. The DMAPS-graft-copolymerized EB film adhered strongly with itself or with other graft copolymerized EB films when brought into close contact in the presence of water and subsequently dried. The adhesive-free adhesion strength is dependent on the graft concentration, the surface microstructure, the nature of the substrate, and the nature of charge-transfer interaction among the graft chains. Finally, respectable adhesive-free adhesion strengths are also obtained between the surface modified EB film and a similarly surface modified PTFE film.

References and Notes

(1) See, for example: Skotheim, T., Ed. *Handbook of Conducting Polymers*; Marcel Dekker: New York, 1986; Vols. I and II.
(2) Green, A. G.; Woodhead, A. E. *J. Chem. Soc.* **1910**, *97*, 2388.
(3) MacDiarmid, A. G.; Chiang, J. C.; Richter, A. F.; Epstein, A. J. *Synth. Met.* **1987**, *18*, 285.
(4) Angelopoulous, M.; Asturias, G. E.; Ertmer, S. P.; Ray, A.; Scherr, E. M.; MacDiarmid, A. G. *Mol. Cryst. Liq. Cryst.* **1988**, *160*, 151.
(5) Andreatta, A.; Cato, Y.; Chiang, J. C.; Heeger, A. J.; Smith, P. *Synth. Met.* **1988**, *26*, 383.
(6) Chiang, J. C.; MacDiarmid; A. G. *Synth. Met.* **1986**, *13*, 193.
(7) Penn, L. S.; Wang, H. *Polym. Adv. Technol.* **1994**, *5*, 809.
(8) Suzuki, M.; Kishida, A.; Iwata, H.; Ikada, Y. *Macromolecules* **1986**, *19*, 804.
(9) Ikada, Y.; Uyama, Y. *Lubricating Polymer Surfaces*; Technomic Publishing Co., Ltd.: Lancaster, PA, 1993.
(10) Tan, K. L.; Woon, L. L.; Wong, H. K.; Kang, E. T.; Neoh, K. G. *Macromolecules* **1993**, *26*, 2832.
(11) Emi, S.; Murase, Y.; Hayashi, T.; Nakajima, A. *J. Appl. Polym. Sci.* **1990**, *41*, 2753.
(12) Liu, S. H.; Ito, Y.; Imanishi, Y. *Biomaterials* **1992**, *13*, 50.
(13) Yamada, K.; Tsutaya, H.; Tatekawa, S.; Hirata, M. *J. Appl. Polym. Sci.* **1992**, *46*, 1068.
(14) Chen, K.-S.; Uyama, Y.; Ikada, Y. *Langmuir* **1994**, *10*, 1319.
(15) Kang, E. T.; Neoh, K. G.; Tan, K. L.; Uyama, Y.; Morikawa, N.; Ikada, Y. *Macromolecules* **1992**, *25*, 1959.

(16) VanDyke, L. S.; Brumlik, C. J.; Liang, W.; Lei, J.; Martin, C. R.; Yu, Z.; Li, L.; Collines, G. J. *Synth. Met.* **1994**, *62*, 75.
(17) Neoh, K. G.; Kang, E. T.; Tan, K. L. *Polym. Degrad. Stab.* **1990**, *27*, 107.
(18) Kang, E. T.; Neoh, K. G.; Zhang, X.; Tan K. L.; Liaw, D. J. *Surf. Interface Anal.* **1996**, *24*, 51.
(19) Kang, E. T.; Kato, K.; Uyama, Y.; Ikada, Y. *J. Mater. Res.* **1996**, *11*, 1570.
(20) Liaw, D. J.; Lee, W. F.; Whung Y. C.; Lin, M. C. *J. Appl. Polym. Sci.* **1987**, *34*, 999.
(21) Kang, E. T.; Neoh, K. G.; Chen, W.; Tan, K. L.; Liaw, D. J.; Huang, C. C. *J. Adhes. Sci. Tech.* **1996**, *10*, 725.
(22) Kang, E. T., Neoh, K. G.; Tan, K. L. *Adv. Polym. Sci.* **1993**, *106*, 135.
(23) Snauwaert, P.; Lazzaroni, J.; Riga, J.; Verbist, J. J.; Gonbeau, D. *J. Chem. Phys.* **1990**, *92*, 2187.
(24) Angelopoulos, M.; Liao, Y. H.; MacDiarmid, A. G.; Zheng, W. G.; Epstein, A. J.; Long, S.; Arbuckle, G. *Proceedings of the ICSM 96*; Snowbird, Utah, Jul 28−Aug 2, 1996; p 150.
(25) Muilenberg, G. E., Ed. *Handbook of X-ray Photoelectron Spectroscopy*; Perkin−Elmer: Eden Prairie, MN, 1992; p 216.
(26) Inagaki, N.; Tanaka, S.; Kawai, H. *J. Polym. Sci., Part A: Polym. Chem.* **1995**, *33*, 2001.
(27) Clark, D. T.; Hutton, D. R. *J. Polym. Sci., Part A: Polym. Chem.* **1987**, *25*, 2643.
(28) Kang, E. T.; Neoh, K. G.; Tan, K. L.; Loh, F. C.; Liaw, D. J. *Polym. Adv. Technol.* **1994**, *5*, 837.
(29) Yamada, K.; Kimura, T.; Tsutaya, H.; Hirata, M. *J. Appl. Polym. Sci.* **1992**, *44*, 993.
(30) Pritchart, H. W. *Acta Polym.* **1983**, *34*, 112.
(31) Voyutskii, S. S. *J. Adhes.* **1971**, *3*, 69.

MA961595E